

## ORIGINAL ARTICLE

## Fundamental Soil Science

# Influence of vegetation type on silicon content in different subtropical soils

Luana Dalacorte<sup>1</sup>  | Ana Paula Rodrigues da Silva<sup>2</sup> | Dirceu Maximino Fernandes<sup>2</sup> | Edson Campanhola Bortoluzzi<sup>1</sup> 

<sup>1</sup>Laboratory of Land Use and Natural Resources, University of Passo Fundo (UPF), Passo Fundo, Rio Grande do Sul, Brazil

<sup>2</sup>College of Agronomic Science Campus Botucatu Department of Forest Science, Soils and Environment, São Paulo State University (UNESP), Botucatu, São Paulo, Brazil

## Correspondence

Edson Campanhola Bortoluzzi, Laboratory of Land Use and Natural Resources, University of Passo Fundo (UPF), Passo Fundo, RS, Brazil.  
Email: [edsonb@upf.br](mailto:edsonb@upf.br)

Assigned to Associate Editor Jonathan Judy.

## Funding information

Conselho Nacional de Desenvolvimento Científico e Tecnológico-CNPq; Productivity in Research Grant, PQ-1D, Grant/Award Number: 302460/2022-5; Coordenação de Aperfeiçoamento de Pessoal de Nível Superior, Grant/Award Numbers: Code 001, PROSUC/CAPES

## Abstract

Soil weathering is the term that describes soil genesis, and its good visual indicators are natural vegetation cover and soil morphology. However, do the same soil types under different vegetation covers affect the degree of soil weathering? Our objective was to study two contrasting soil types under natural vegetation to discuss the degree of weathering, considering their morphology, silicon (Si) content, and fine mineralogy assemblage. Soil samples were collected in nearby Brazilian regions with Ferralsol and Regosol soils, as well as native forest and grassland areas. Soil profile, mineralogy, and chemical composition (total and available ions) were described. Both soils presented the following minerals: mica/illite, kaolinite, quartz, and cristobalite. Available Si content ranged from 6.31 to 8.76 mg kg<sup>-1</sup>, and it was higher in Ferralsol than in Regosol soils but did not show dependency on the vegetation type. The total SiO<sub>2</sub> content ranged from 283.5 to 341.4 g kg<sup>-1</sup>. The Ki index was higher in the A horizons (2.77) of Ferralsols than in Regosols. The silt/clay ratio content discriminated soil types more accurately. Although vegetation types, mineralogy effects, and Si availability were weak as factors of soil evolution under native conditions, these findings do not end the discussion about the impact of vegetation cover on soil weathering. Further studies on different soil classes are recommended, including assessments of Si content in plant tissues, to elucidate the link of vegetation and mineralogy to chemical availability.

## Plain Language Summary

Soil vegetation cover is a factor agent for soil development and evolution (weathering). The study objective was to take contrast soil types under two natural vegetation types to discuss soil weathering aspects. Concerning soil morphology, silicon concentrations, and mineralogical composition, vegetation types played a limited role in soil evolution under native conditions.

**Abbreviations:** ADFE, air-dried fine earth fraction; FNF, Ferralsol under native forest; FNG, Ferralsol under native grassland; RNF, Regosol under native forest; RNG, Regosol under native grassland; XRD, x-ray diffraction; XRF, x-ray fluorescence.

This is an open access article under the terms of the [Creative Commons Attribution](https://creativecommons.org/licenses/by/4.0/) License, which permits use, distribution and reproduction in any medium, provided the original work is properly cited.

© 2025 The Author(s). *Soil Science Society of America Journal* published by Wiley Periodicals LLC on behalf of Soil Science Society of America.

## 1 | INTRODUCTION

Soils are heterogeneous, and this heterogeneity may be inherited from the parent material, acquired through pedogenic processes, or both. It may also be directly influenced by vegetation. Thus, soils are formed through constructive and destructive processes and are composed of rock and mineral particles that have been fragmented and altered by weathering, which changes the chemical and mineralogical state of these components across spatial and temporal dimensions (Pujar et al., 2012; Tale & Ingole, 2015).

The degree of soil weathering is mostly estimated through morphological characteristics (Churchman & Lowe, 2012). However, total silicon (Si) and other total cations (i.e., iron [Fe], aluminum [Al], titanium [Ti], calcium [Ca], magnesium [Mg], and potassium [K]) may represent parameters for calculating soil genesis indices, such as the weathering intensity scale (Meunier et al., 2007, 2013) and chemical iron index (Ki) and chemical weathering index (Kr). The secondary mineral assemblage in soils is expected to be determined by the level of available ions, such as Si, Al, and Fe, after the weathering process. For instance, available Si is rapidly lost in well-drained soils, such as Oxisols, due to their high degree of weathering. That occurs because high temperatures and water flux promote the general desilication process of clay-sized minerals (White et al., 2012; Zabowski & Ugolini, 1992). Si is an abundant element in the Earth's crust, and it is little relevant as a nutrient for higher plants (da Silva et al., 2023; Deus et al., 2024). However, this element effectively alleviates abiotic and biotic stresses in plant cultures (Mamasolieva et al., 2024).

The Si in soils may appear in different chemical associations but predominantly in secondary clay minerals and biogenic forms (Tubana et al., 2016). Lithogenic minerals undergo weathering followed by desilication (Si leaching) through the hydrolysis mechanism, a process that renders soils poor in Si. The literature reports that approximately 3.5 billion ha of land worldwide is Si-deficient. Low levels of available Si are common in Ferralsols and Arenosols, for instance, due to the high degree of weathering experienced by these soils (De Tombeur et al., 2021).

Plants are also relevant in Si cycling in soils. The literature reports that since the Cenozoic era, over 400 million years ago, grasses and diatoms have controlled the biological Si cycle (Cermeño et al., 2015). The absorption of aqueous substances by plants also partially controls soil formation through their impact on soil solution chemistry, which can influence the bioavailability of Si in soils (Blecker et al., 2006; Henriët et al., 2008). Another portion of Si may be absorbed by plants and accumulated as phytoliths (Ashfaq et al., 2024; De Tombeur et al., 2021; Puppe et al., 2023). Plant species have different capacity levels for Si accumulation (Ahmed

### Core Ideas

- The impact of vegetation on the degree of soil weathering is still poorly understood.
- The studied soils share similar mineralogical characteristics, regardless of their degree of weathering and morphology.
- Vegetation type does not influence the concentration of available silicon in the studied soils.

et al., 2023; Strömberg et al., 2016). Thus, the community of species may drive Si dynamics and consequently alter mineral assemblage (Korchagin et al., 2019; Zaman et al., 2025). In controlled experimental conditions, plant species accelerate the cation release rate, including the loss of Si, Ca, and sodium (Na), which suggests mineral dissolution (Hinsinger et al., 2001).

However, in field conditions, such as different biomes, vegetation should regulate Si dynamics according to the soil mineral assemblage, an aspect still scarcely described in the literature. That is the primary interest in the South Brazilian subtropical region, where the Pampa's forests and prairies cohabit on similar soil types. Thus, we hypothesize that the Si content and mineral assemblage vary with soil types and vegetation covers.

In this sense, this study aimed to examine the morphological, chemical, and mineralogical attributes, including available Si, on different soil types (Ferralsol and Regosol) within two vegetation covers (grassland and forest). These findings will help elucidate the association of the degree of weathering with several traits, especially in subtropical soils where the two biomes coexist.

## 2 | MATERIALS AND METHODS

### 2.1 | Site description and soil sample collection

The climate of Água Santa, Rio Grande do Sul, Brazil, is subtropical humid (Cfa) according to the Köppen–Geiger classification (Alvares et al., 2013). The average temperature is 20.6°C, and the average annual precipitation is 1409 mm. The geology of the Paraná Basin is volcanism (Mesozoic era), and it is known as the Serra Geral Formation in the study region. This formation comprises ~90% basalt and 2%–5% rhyolite and rhyodacite (acid rocks). Sedimentary rocks (sandstone) may appear locally on the surface, even though they are older rocks (Nardy et al., 2002). Petrographically, the rocks from the Serra Geral Formation comprise



**FIGURE 1** Map of soil collection locations. The sites were Ferralsol under native grassland (FNG) (1) and native forest (FNF) (2), and Regosol under native grassland (RNG) (3) and native forest (RNF) (4).

plagioclase (60%–65%), clinopyroxene, and alkali feldspars (Gómez et al., 2010). Caner et al. (2014) and Bortoluzzi et al. (2015) provide a detailed soil gradient mineralogy from different rock types.

The Água Santa municipality coexists with the Atlantic Forest biome and native grassland (Pampa biome) in a smooth relief (IBGE, 2019). Thus, two sites were selected (Figure 1) and had their soils classified based on morphological attributes (Table 1).

The first location is represented by the Pampa biome (Campos Gerais plateau), which comprises native rangelands across several countries in South America, mainly in Brazil, Uruguay, and Argentina. Estimations show that less than 25% of the original biome remains (Oliveira et al., 2017). The primary genera from the Pampa biome are *Paspalum* sp., *Axonopus* sp., *Andropogon* sp., *Eryngium*, and *Baccharis* sp. (Boldrini, 1997). These rangelands present seasonality in forage production, which is abundant in spring–summer seasons and scarce in autumn–winter. The second site is represented by the Mixed Ombrophilous Forest (MOF), which is the southern part of the Atlantic Forest. The MOF is home to the *Araucaria*, a native conifer that dominates the upper stratum, as well as species of the Myrtaceae, Fabaceae, Lauraceae, and Euphorbiaceae families in the lower stratum (Passos et al., 2021).

This study employed descriptions of soil morphology attributes, by the Brazilian Institute of Geography and Statistics (IBGE, 2015), and their physical properties by Teixeira et al. (2017). Soil profiles were classified according to the soil taxonomy (Soil Survey Staff, 2022) and the World Reference Base (IUSS Working Group WRB, 2022) (Table 1).

Concerning the chemical composition of soils (Table 2), soil samples were collected from the A and Bw horizons for Ferralsols and from the A horizon for Regosols. The following parameters were evaluated: water pH, exchangeable  $\text{Ca}^{2+}$ ,  $\text{Mg}^{2+}$ ,  $\text{Al}^{3+}$ , K, P, hydrogen (H) + Al, and organic matter (Teixeira et al., 2017).

## 2.2 | Experimental design

The survey was conducted in four field conditions (two soil types and two vegetation covers): Ferralsol under native grassland (FNG) and native forest (FNF), and Regosol under native grassland (RNG) and native forest (RNF). Trenches were dug in the fields using an excavator, and soil samples comprising five subsamples were collected in the A horizons (0–20 cm layer) and the middle of Bw horizons for Ferralsols. The soil samples were dried at room temperature and sieved through a 2-mm sieve to obtain the air-dried fine earth fraction (ADFE).

## 2.3 | Analyzed variables

### 2.3.1 | Available Si in soils

Colorimetry was applied to determine Si after extraction with  $0.01 \text{ mol L}^{-1} \text{ CaCl}_2$ , as per Korndörfer et al. (2004). An aliquot of 10 g of ADFE (<2-mm fraction) was placed in a 150-mL flask, which was filled with 100 mL of the extracting solution. Additionally, a standard sample was taken. Next, 1 mL of the sulfomolybdic acid solution was added to each sample. After 10 min, 2 mL of tartaric acid solution ( $200 \text{ mg L}^{-1}$ ) was introduced, followed by the addition of 10 mL of the ascorbic acid solution after a further 5 min. After 1 h, a UV-visible spectrophotometer operating at a 660 nm wavelength performed the measurements.

### 2.3.2 | Analysis of total chemical composition of the clay fraction: Focus on Si, Al, Fe, and Ti

The following pretreatments utilized an aliquot of 40 g of ADFE, according to Bortoluzzi and Poletto (2013): (i) organic matter elimination using 5% v/v of hydrogen peroxide, (ii) chemical dispersion ( $0.1 \text{ mol L}^{-1} \text{ NaOH} + 0.07 \text{ mol L}^{-1} \text{ NaPO}_3$ ) and mechanical dispersion by a horizontal stirring table (16 h), and (iii) granulometric separation occurred by the sedimentation and pipette method (Gee & Bauder, 1986). The >0.053-mm fraction (sand fraction) was separated by sieving, while silt and clay fractions (<0.002 mm) were separated by the pipette method. All fraction sizes were dried at room temperature.

Aliquots of 10 g of the dry clay fraction were pressed at 20 metric tonnes, forming pellets, and submitted to dispersive-energy x-ray fluorescence (XRF) (Bortoluzzi & Poletto, 2013). The XRF device was an S2 Ranger from Bruker, operating with a maximum power generator at a voltage of 50 W, a current intensity of 2 mA, and an x-ray tube made of anode material (Pd-lead). Total Si, Al, Fe, and Ti concentrations were measured in five replicates, and their averages were expressed as oxides.

The XRF results enabled the calculation of the  $K_i$ ,  $K_r$ , and productivity indices (Teixeira & Campos, 2017) using the following equations:

$$K_i = \text{SiO}_2 / \text{Al}_2\text{O}_3 \times 1.07$$

$$K_r = (\text{SiO}_2 / 0.6) / ([\text{Al}_2\text{O}_3 / 1.02] + [\text{Fe}_2\text{O}_3 / 1.6])$$

$$\text{Productivity index} = (100) \left( \text{SiO}_2 / [\text{TiO}_2 + \text{Fe}_2\text{O}_3 + \text{Al}_2\text{O}_3 + \text{SiO}_2] \right) \text{ (Demir et al., 2022)}$$

where silicon dioxide ( $\text{SiO}_2$ ), aluminum oxide ( $\text{Al}_2\text{O}_3$ ), iron oxide ( $\text{Fe}_2\text{O}_3$ ), and titanium oxide ( $\text{TiO}_2$ ) were expressed in  $\text{g kg}^{-1}$ .

$K_i$  represents the relative amounts of silica housed in less weathered minerals and Al associated with  $\text{Fe}_2\text{O}_3$  (stable minerals). High  $K_i$  values suggest less weathering and an abundance of less weathered minerals.  $K_r$  represents the ratio between Si and the sum of Al and Fe. High  $K_i$  values suggest high weathering and an abundance of highly weathered minerals (Teixeira & Campos, 2017). Demir et al. (2022) stated that the productivity index represents the proportion of Si to a total of other cations, a valuable indicator for the degree of weathering.

### 2.3.3 | Mineralogical characterization

Silt and clay fractions underwent equivalent mineralogical characterizations using a Bruker D2 Phaser x-ray diffraction (XRD) device—Cu radiation. The methodology followed the work by Bortoluzzi and Poletto (2013). In summary, the fractions were prepared according to the pretreatments: (i) one Ca-saturated (CaCl) aliquot and a second K-saturated (KCl) aliquot, and (ii) washing the suspensions to obtain the salt-free aliquots of silt and clay fractions.

The samples were placed onto glass slides in an oriented way and air-dried (AD) at room temperature, and the slides underwent the following treatments: (i) air-drying Ca-saturated samples and recording XRD patterns between  $3^\circ$  and  $28^\circ 2\theta$  (Ca-AD); (ii) recording XRD patterns between  $3^\circ$  and  $28^\circ 2\theta$  after solvation with ethylene glycol (Ca-EG); and (iii) recording K-saturated samples in XRD between  $3^\circ$  and  $28^\circ 2\theta$  after heating at temperatures of  $150^\circ\text{C}$  (K- $150^\circ\text{C}$ ),  $350^\circ\text{C}$  (K- $350^\circ\text{C}$ ), and  $550^\circ\text{C}$  (K- $550^\circ\text{C}$ ) using a muffle furnace. The 001 peaks in XRD patterns were identified by comparison using the key found in Brown and Brindley (1980).

## 2.4 | Statistical analyses

The quantitative data (i.e., available and total cations and weathering indices) underwent a one-way analysis of variance. Significant values were further analyzed using Tukey's test at  $p < 0.05$  in Agroestat software.

## 3 | RESULTS

### 3.1 | Weathering indicators: Available Si, Fe, and Al oxides

The available Si content in the study areas ranged from 6.31 to  $8.76 \text{ mg kg}^{-1}$ . They were higher in Ferralsol and did not

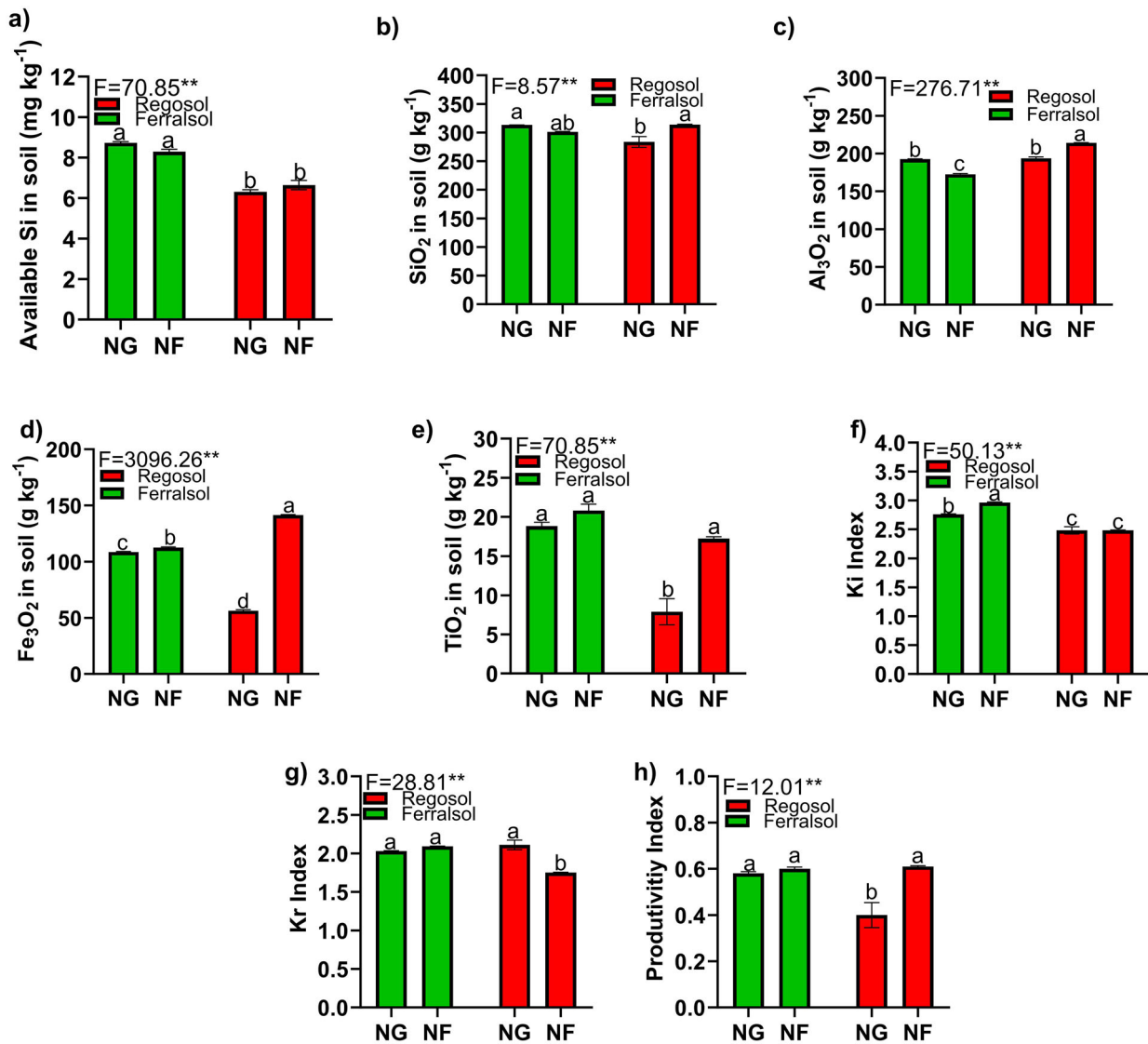


**FIGURE 2** Available silicon (a), total silicon (SiO<sub>2</sub>) (b), total aluminum (Al<sub>2</sub>O<sub>3</sub>) (c), total iron (Fe<sub>2</sub>O<sub>3</sub>) (d), and total titanium (TiO<sub>2</sub>) (e) oxides, and chemical iron index (Ki) (f), chemical weathering index (Kr) (g), and productivity index (h) of the clay fraction from Ferralsol and Regosol developed in natural areas (grassland and forest). *F* values followed by \*\* are significant at 5% of error. Means followed by the same letter in the column did not differ statistically by Tukey's test at 5% probability. Error bars represent the standard error ( $n = 5$ ). Ki, Kr, and productivity indices originated from the clay fraction. NF, native forest; NG, native grassland.

significantly influence vegetation type. The acid rock type may partially explain the dystrophic character, with a low sum of cations (K, Ca, and Mg) from both soils (Gómez et al., 2010). In contrast, the available Si content in Regosol areas was lower, regardless of the vegetation type (Figure 2a). The total chemical content ranged from 283.5 to 341.4 g kg<sup>-1</sup> for SiO<sub>2</sub>, 172.63 to 214.33 g kg<sup>-1</sup> for Al<sub>2</sub>O<sub>3</sub>, 56.33 to 141.4 g kg<sup>-1</sup> for Fe<sub>2</sub>O<sub>3</sub>, and 7.90 to 20.8 g kg<sup>-1</sup> for TiO<sub>2</sub> (Figure 2b-e). Silicon dioxide (SiO<sub>2</sub>) concentrations were higher in Ferralsol under grassland and RNF. Regosol under grassland presented the lowest SiO<sub>2</sub> concentration (Figure 2b).

The concentrations of aluminum (Al<sub>2</sub>O<sub>3</sub>) and iron (Fe<sub>2</sub>O<sub>3</sub>) oxides were higher in RNFs (Figure 2c,d). Ferralsol in the for-

est area showed the lowest Al<sub>2</sub>O<sub>3</sub> concentration. Both soils under grassland had similar average values (Figure 2c). RNG had the lowest average Fe<sub>2</sub>O<sub>3</sub> concentration, followed by Ferralsol under the same vegetation type (Figure 2d).

TiO<sub>2</sub> concentrations were similar in Oxisol, regardless of the vegetation covering the soil, and did not differ from the TiO<sub>2</sub> concentration in RNF. RNG presented the lowest average concentration of this element (Figure 2e).

The Ki index was higher in the A horizon (2.77) of Ferralsols. The vegetation cover influenced Ki values, as FNF had the highest value (2.97) compared to FNG. Additionally, FNF had a higher Ki index than the grassland. This index was similar (2.49) for Regosol, regardless of the vegetation (Figure 2f). Conversely, the Kr index showed higher averages for all A

horizons from both soils (Ferralsol and Regosol), except for RNF, which exhibited the lowest Kr index (Figure 2g). The productivity index was near 1.0 for Ferralsol, regardless of the vegetation. As for Regosol, this index was higher than 1.0 under grass (1.11) and lower than 1.0 under forest (0.84) (Figure 2h).

### 3.2 | Mineralogical analysis of the soil

The mineralogical assemblage from clay and silt fractions was similar between the two soil weathering types (Ferralsol and Regosol) (Figures 3 and 4). Ferralsol under two native vegetation covers (FNG and FNF) presented the following minerals: illite ( $d = 1.001$  nm), kaolinite ( $d = 0.716$  nm;  $d = 0.357$  nm), quartz ( $d = 0.425$  nm;  $d = 0.334$  nm), and cristobalite ( $d = 0.405$  nm) (Figure 3). The clay fraction in the mineralogical assemblage of RNG and RNF exhibited the following minerals: illite ( $d = 1.001$  nm), kaolinite ( $d = 0.716$  nm;  $d = 0.357$  nm), quartz ( $d = 0.425$  nm;  $d = 0.334$  nm), and cristobalite ( $d = 0.405$  nm) (Figure 3).

The mineralogical assemblage of FNG and FNF silt fraction presented the following predominant minerals: quartz ( $d = 0.425$  nm;  $d = 0.334$  nm) and cristobalite ( $d = 0.405$  nm) (Figure 4). The mineralogical assemblage of RNG and RNF silt fraction showed the following minerals from native grassland and forest: quartz ( $d = 0.425$  nm;  $d = 0.334$  nm) and cristobalite ( $d = 0.405$  nm) (Figure 4). Additionally, tridymite ( $d = 0.410$  nm) and traces of kaolinite ( $d = 0.716$  nm) were found in RNG.

## 4 | DISCUSSION

Ferralsols are predominantly red, deep, highly weathered, and rich in kaolinite and sesquioxides of Fe and Al (De Oliveira et al., 2020). Regosols are morphologically less weathered, do not have a B horizon, and present rich 2:1 clay mineralogy (Bortoluzzi et al., 2012). Morphologically, the studied soils are markedly different, and their morphological traits are consistent with the expectations for Ferralsols (deep and red profile) and Regosols (weak profile without a B horizon). Our study showed that Ferralsol presented higher available Si concentrations, while Regosol presented the lowest averages, regardless of the vegetation (Figure 2a). This scenario may be due to the soil texture (Table 1), as clayey soils have higher soluble Si concentrations (Demattê et al., 2011). Thus, it is expected that Ferralsol, presenting a clay texture, would have more available Si than Regosol, which presents half the clay fraction content. Moreover, the bedrock from this region predominantly comprises basalt and rhyodacite (Gomez et al., 2010). Thus, the different textures of the studied soils resulted from the degrees of weathering. Demir et al.

(2022) stated that different weathering degrees are associated with volcanic rocks.

The fact that silicon oxide ( $\text{SiO}_2$ ) concentrations in RNFs were similar to those in Ferralsol under grassland did not influence soluble Si concentrations. These data suggest that it is not always possible to correlate total Si concentrations with available Si, as its release into a solution depends on several factors, such as the degree of weathering these soils have undergone and their adsorption capacity (Deus et al., 2024). The literature reports that plants control Si biological cycles (Cermeño et al., 2015). The Si absorbed by plants may influence its bioavailability in soils and accumulation in tissue phytoliths (Ashfaq et al., 2024; Blecker et al., 2006; De Tombeur et al., 2021; Henriot et al., 2008; Puppe et al., 2023). Grassland species have high Si accumulation capacities because they belong to the Poaceae family (Ahmed et al., 2023; Strömberg et al., 2016; Zaman et al., 2025). Although plants accelerate Si loss through mineral dissolution (Hinsinger et al., 2001; Korchagin et al., 2019), the native vegetation regulates Si dynamics, recycling it and sinking it into biomaterials (Puppe et al., 2023).

The Regosol from the forest area showed the highest  $\text{Fe}_3\text{O}_2$  and  $\text{Al}_3\text{O}_2$  concentrations (Figures 2c,d), while  $\text{TiO}_2$  values were different only in RNG. The higher concentrations of  $\text{Fe}_3\text{O}_2$ ,  $\text{Al}_3\text{O}_2$ , and  $\text{TiO}_2$  in Regosol under the forest area are likely related to the degree of weathering this soil has experienced. The Ki and Kr indices are valuable indicators of the degree of weathering in contrasted soils covered by different vegetation types (Schaetzl & Anderson, 2005). In this study, Ki and Kr values were higher, with  $>2.5$  for Ki and  $>1.7$  for Kr. A Kr value near 1.76–2 indicated kaolinitic soils. Both soil types (Ferralsol and Regosol) presented high Ki indices, indicating a low degree of weathering despite Ferralsol being a highly weathered soil. The literature reports that Ki values near 2.5 and Kr near 2.0 indicate the predominance of 1:1 phyllosilicate,  $\text{Fe}_3\text{O}_2$ , and  $\text{Al}_3\text{O}_2$  in the clay fraction (Curi & Kämpf, 2012; Guimarães et al., 2021). The productivity index values confirm this interpretation (Demir et al., 2022). Quantitatively, the silt/clay ratios remained lower than 1.0 for Ferralsols and higher than 1.0 for Regosols (Table 1). The highest ratio occurred in RNG (2.08). The silt/clay ratio is an auxiliary index to indicate the degree of soil weathering. The silt fraction is a good auxiliary indicator for discriminating soil weathering (Aquino et al., 2016). Higher values indicate a low degree of weathering for the Regosol, while a high degree of weathering may be due to the low silt fraction in Ferralsols.

Several factors influence weathering processes, including rainfall regime, temperature variations, and wind (Guimarães et al., 2021; Stockmann et al., 2014). The region where the studied soils developed has a cooler and more humid climate than other areas with Latosols in Brazil, which may decrease the weathering process. Thus, the mineral assemblage of the soils, with the predominance of kaolinite, was consistent with

TABLE 1 Sample locations and main morphological properties of soils developed in natural areas.

Soil type/Soil use <sup>a</sup>	Horizon (cm)	Munsell color wet	Structure	Consistency		Moist	Sand (g kg <sup>-1</sup> )	Silt (g kg <sup>-1</sup> )	Clay (g kg <sup>-1</sup> )	Texture classes
				Dry	Wet					
Ferralsol/Oxisol										
Native grassland	A 0–40	7.5YR 3/2	Subangular blocky	Hard	Friable	Plastic sticky	343.1	178.6	478.2	Clay
28°16'0.4" S; 52°1'57" W 740 m	AB 40–70	7.5YR 3/3	Subangular blocky	Hard	Friable	Plastic sticky	–	–	–	–
	Bw 70–130	7.5YR 3/4	Subangular blocky	Hard	Friable	Plastic sticky	162.63	323.90	513.47	Clay
	C 130+	–	–	–	–	–	–	–	–	–
Ferralsol/Oxisol										
Native forest	A 0–40	7.5YR 3/1	Granular	Slightly hard	Very friable	Slightly plastic and sticky	305.56	224.36	470.09	Clay
28°16'3.4" S; 52°1'58" W 755 m	AB 40–70	7.5YR 3/2	Subangular blocky	Slightly hard	Very friable	Slightly plastic and sticky	–	–	–	–
	Bw 70–140	7.5YR 3/3	Subangular blocky	Hard	Friable	Plastic sticky	181.87	238.82	579.31	Clay
	C 140+	–	–	–	–	–	–	–	–	–
Regoso/Entisol										
Native grassland	A 0–15	7.5YR 3/2	Subangular blocky	Slightly hard	Very friable	Slightly plastic and sticky	333.82	449.71	216.47	Loam
28°16'0.1" S; 52°1'55" W 741 m	C 15+	–	–	–	–	–	–	–	–	–
Regoso/Entisol										
Native forest	A 0–13	7.5YR 3/1	Granular	Slightly hard	Very friable	Slightly plastic and sticky	249.54	392.23	358.22	Clay loam
28°16'5.4" S; 52°1'58" W 758 m	C 13+	–	–	–	–	–	–	–	–	–

<sup>a</sup>Geographical coordinates. Soil description based on FAO (2006) and IUSS Working Group WRB (2022). Data not collected.

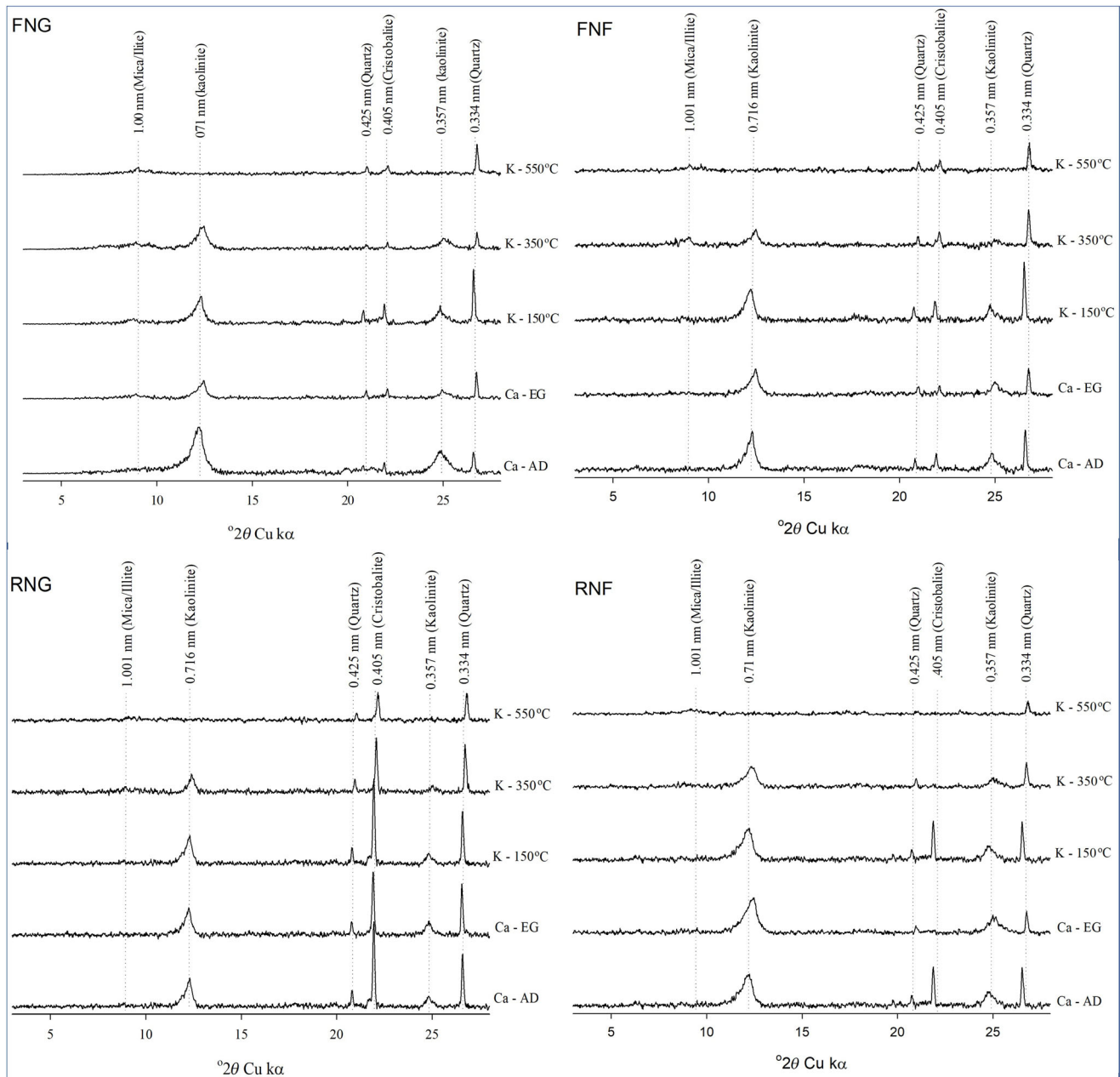


**FIGURE 3** x-Ray diffraction patterns of the clay fraction of Ferralsol under native grassland (FNG) and native forest (FNF) and Regosol under native grassland (RNG) and native forest (RNF) by the following pretreatments: AD (air-dried); EG (ethylene glycol solvation); and K-150°C (K-saturated and heated at 150°C), K-350°C (K-saturated and heated at 350°C), and K-550°C (K-saturated and heated at 550°C).

these climatic conditions (Figures 3 and 4). However, the clay fraction composition was also based on the presence of illite, quartz, cristobalite, and Fe and Al sesquioxides. The mineral assemblage presented few differences between the vegetation covers. However, all XRD patterns exhibited weak peaks corresponding to muscovite/illite, a K-2:1 interlayer clay mineral, indicating low amounts of this clay mineral in both soil types and vegetation covers. However, 2:1 clay minerals associated with oxide minerals are found in highly weathered soils, including in southern Brazil (Arkcoll et al., 1985; Bortoluzzi et al., 2015; Bortoluzzi, Pernes, et al., 2008; Bortoluzzi, Velde, et al., 2008; Melo et al., 2002, 2003). A

plausible explanation is that mica/illite clay minerals are thermodynamically stable and may remain during the weathering process in some regions (Alves et al., 2013). Therefore, 2:1 clay minerals (minerals rich in chemical products) may be found associated with highly weathered soils composed of oxide mineralogy (Bhattacharyya et al., 2000). The mineral assemblage in both soil and vegetation types containing 2:1 clay minerals may explain the relatively high cation exchange capacity values (Table 2).

The silt fraction of Ferralsol exhibited predominantly primary minerals, such as quartz and cristobalite, and did not qualitatively differ between vegetation covers. The silt

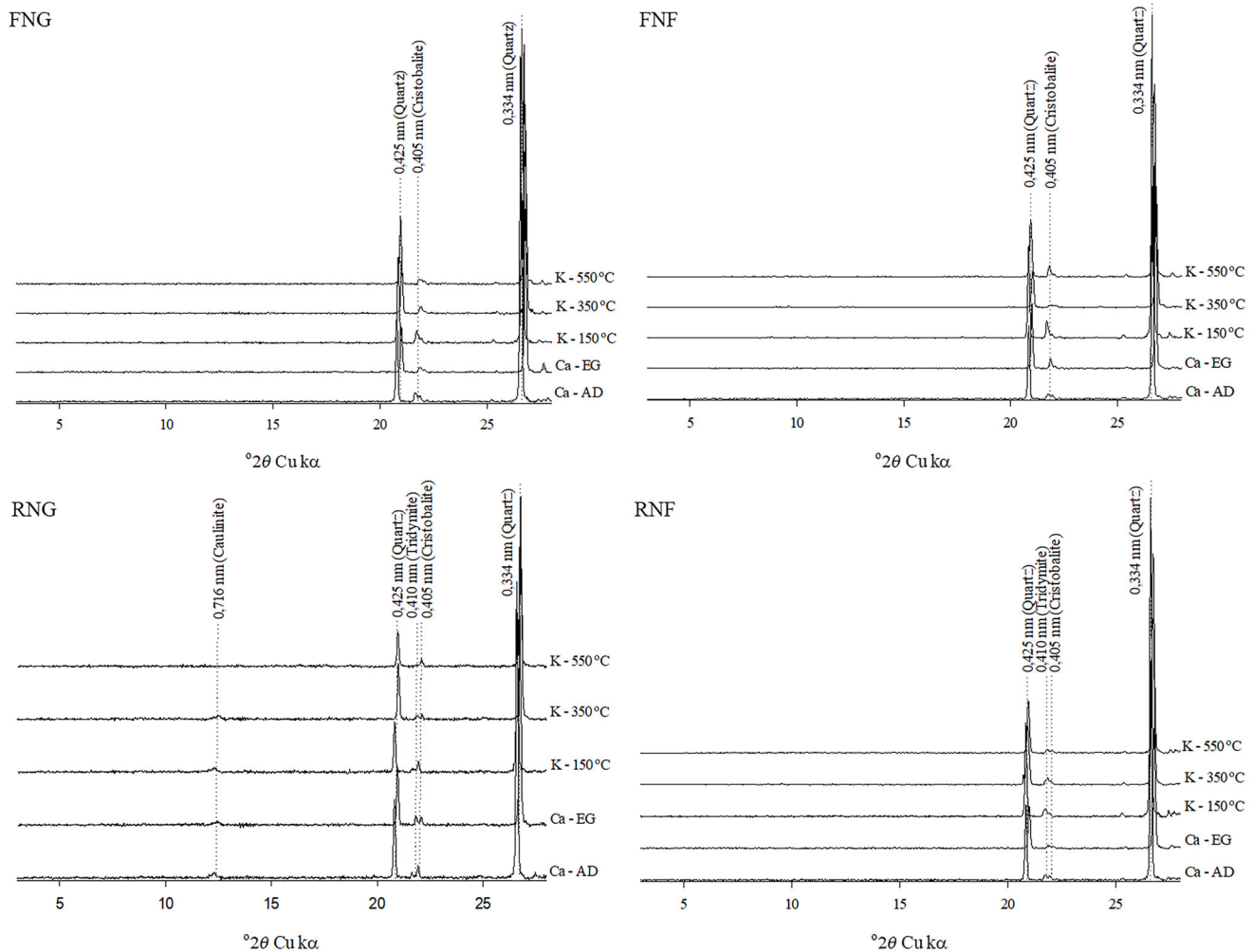


**FIGURE 4** x-Ray diffraction patterns of the silt fraction of Ferralsol under native grassland (FNG) and native forest (FNF) and Regosol under native grassland (RNG) and native forest (RNF) by the following pretreatments: AD (air-dried); EG (ethylene glycol solvation); and K-150°C (K-saturated and heated at 150°C), K-350°C (K-saturated and heated at 350°C), and K-550°C (K-saturated and heated at 550°C).

fraction of Regosol included kaolinite, quartz, tridymite, and cristobalite, and the vegetation cover showed differences only in the presence of kaolinite. In summary, the mineral set is predominantly similar to the original parent material and climate, as suggested by Stockmann et al. (2014).

The present study suggests a close relationship between a similar mineral assemblage and the climatic regime and bedrock type, even presenting soil profiles with morphological contrast (Table 1). The provided data raise a question about the most sensitive indicator for discriminating the degree of soil weathering or the potential weathering rate evaluation using a group of morphological, chemical, physical, and mineralogical attributes. This study balanced several soil attributes and provided a valuable discussion of soil genesis occurrence under the same climatic conditions but with different native vegetation. Isolated attributes, such as mineral assemblage, seem insufficient to indicate the degree of soil weathering. We observed a disruptive interpretation between mineralogy and soil morphological characteristics and weath-

ering indices. However, the changes in mineral assemblage become evident when replacing the natural vegetation with exotic species that are aggressive and capable of altering their environment to absorb nutrients and water (Hummes et al., 2024; Korchagin et al., 2019). Ehrenfeld et al. (2005) warn about evidence of plant–soil system feedbacks, which present a complex interaction and must be considered for elucidating the soil formation process.

## 5 | CONCLUSION

The analyzed region presents an odd condition, as it is the interface between two main biomes under a subtropical climate (Pampa and MOF, a subtype of the Atlantic Forest). Thus, the study highlighted differences regarding morphological, chemical, and mineralogical aspects of contrasted weathered soils (Ferralsol and Regosol) under two vegetation types (grassland and forest).

TABLE 2 Chemical properties of two soils under natural vegetation cover.

	Horiz.	pH	H <sub>2</sub> O	Ca <sup>2+</sup> (cmol <sub>c</sub> kg <sup>-1</sup> )	Mg <sup>2+</sup> (cmol <sub>c</sub> kg <sup>-1</sup> )	K <sup>+</sup> (cmol <sub>c</sub> kg <sup>-1</sup> )	SB (cmol <sub>c</sub> kg <sup>-1</sup> )	H <sup>+</sup> (cmol <sub>c</sub> kg <sup>-1</sup> )	Al <sup>3+</sup> (cmol <sub>c</sub> kg <sup>-1</sup> )	H + Al (cmol <sub>c</sub> kg <sup>-1</sup> )	CEC (cmol <sub>c</sub> kg <sup>-1</sup> )	OM (g kg <sup>-1</sup> )	P (mg kg <sup>-1</sup> )
Ferralsol													
	A	4.68	1.46	0.44	0.19	0.19	2.09	0.44	2.20	2.64	4.72	20.88	4.86
Native forest grassland													
	A	4.9	2.30	0.72	0.24	0.24	3.25	0.35	1.74	2.08	5.34	21.26	10.08
Regosol													
	A	5.26	4.02	1.08	0.28	0.28	5.39	0.09	0.46	0.55	5.94	27.20	4.36
	A	4.48	2.12	1.11	0.45	0.45	3.67	0.71	3.54	4.25	7.92	22.04	10.87

Abbreviations: CEC, cation exchange capacity; Horiz., horizon; OM, organic matter; P, Mehlich-1; SB, sum of Ca + Mg + K.

First, the morphological traits were consistent with the expectations for the contrasted soil classes: Ferralsols (deep and red profile) and Regosols (weak profile without a B horizon). However, the fine mineralogy assemblage from soils remains remarkably similar, regardless of the vegetation. Although it was initially anticipated that vegetation would affect Si availability and soil mineralogy, the data indicated that vegetation effects were insignificant in the studied environment. The weathering indices (Ki, Kr, and productivity) provide a similar degree of weathering, regardless of the soil. The silt/clay ratio is possibly more accurate in distinguishing between soil classes.

Finally, this research suggests that understanding Si dynamics in subtropical soils requires higher emphasis on soil type, the presence of specific oxides, and weathering indices rather than solely on vegetation. Additionally, the weathering degree estimation should not be limited to a few indicators, as it involves a large dataset of attributes. Future research should also incorporate vegetation-related data, such as Si content in plant tissue, to explore potential correlations to mineralogy and available concentrations of Si in the soil.

## AUTHOR CONTRIBUTIONS

**Luana Dalacorte:** Conceptualization; formal analysis; writing—original draft. **Ana Paula Rodrigues da Silva:** Visualization; writing—review and editing. **Dirceu Maximino Fernandes:** Visualization; writing—review and editing. **Edson Campanhola Bortoluzzi:** Conceptualization; funding acquisition; project administration; resources; writing—review and editing.

## ACKNOWLEDGMENTS

This study was supported by the Brazilian Coordination for the Improvement of Higher Education Personnel (CAPES) through the Prosuc/CAPES fellowship accorded to Luana Dalacorte and the Brazilian Council for Scientific and Technological Development—CNPq for the fellowship granted to Edson Campanhola Bortoluzzi (CNPq—Brazil: 302460/2022-5).

The Article Processing Charge for the publication of this research was funded by the Coordenação de Aperfeiçoamento de Pessoal de Nível Superior - Brasil (CAPES) (ROR identifier: 00x0ma614).

## ORCID

**Luana Dalacorte**  <https://orcid.org/0000-0002-4503-7283>  
**Edson Campanhola Bortoluzzi**  <https://orcid.org/0000-0002-0967-0057>

## REFERENCES

- Ahmed, S. R., Anwar, Z., Shahbaz, U., Skalicky, M., Ijaz, A., Tariq, M. S., Zulfiqar, U., Brestic, M., Alabdallah, N. M., Alsubeie, M. S., Mujtaba, H., Saeed, A. M., Zahra, T., Hasan, M. D. M., Firdous,

- H., Razaq, A., & Zafar, M. M. (2023). Potential role of silicon in plants against biotic and abiotic stresses. *Silicon*, *15*, 3283–3303. <https://doi.org/10.1007/s12633-022-02254-w>
- Alvares, C. A., Stape, J. L., Sentelhas, P. C., De Moraes Gonçalves, J. L., & Sparovek, G. (2013). Köppen's climate classification map for Brazil. *Meteorologische Zeitschrift*, *22*(6), 711–728. <https://doi.org/10.1127/0941-2948/2013/0507>
- Alves, M. J. F., Melo, V., Reissmann, C. B., & Kaseker, J. F. (2013). Reserva mineral de potássio em Latossolo cultivado com *Pinus taeda* L. *Revista Brasileira de Ciência do Solo*, *37*, 1599–1610. <https://doi.org/10.1590/S0100-06832013000600016>
- Aquino, R. E. D., Marques, J., Campos, M. C. C., Oliveira, I. A. D., Bahia, A. S. R. D. S., & Santos, L. A. C. D. (2016). Characteristics of color and iron oxides of clay fraction in Archeological Dark Earth in Apuí region, southern Amazonas. *Geoderma*, *262*, 35–44. <https://doi.org/10.1016/j.geoderma.2015.07.010>
- Arkcoll, D. B., Goulding, K. W. T., & Hughes, J. C. (1985). Traces of 2:1 layer-silicate clays in Oxisols from Brazil, and their significance for potassium nutrition. *Journal of Soil Science*, *36*(1), 123–128. <https://doi.org/10.1111/j.1365-2389.1985.tb00317.x>
- Ashfaq, W., Brodie, G., Fuentes, S., Pang, A., & Gupta, D. (2024). Silicon improves root system and canopy physiology in wheat under drought stress. *Plant and Soil*, *502*, 279–296. <https://doi.org/10.1007/s11104-023-06202-4>
- Bhattacharyya, T., Pal, D. K., & Srivastava, P. (2000). Formation of gibbsite in the presence of 2:1 minerals: An example from Ultisols of northeast India. *Clay Minerals*, *35*(4), 827–840. <https://doi.org/10.1180/000985500547269>
- Blecker, S. W., McCulley, R. L., Chadwick, O. A., & Kelly, E. F. (2006). Biologic cycling of silica across a grassland bioclimate sequence. *Global Biogeochemical Cycles*, *20*(3), Article GB3023. <https://doi.org/10.1029/2006GB002690>
- Boldrini, I. I. (1997). Campos do Rio Grande do Sul: Caracterização fisionômica e problemática ocupacional. *Boletim do Instituto de Biociências*, *56*, 1–39.
- Bortoluzzi, E. C., Moterle, D. F., Rheinheimer, D. S., Casali, C. A., Melo, G. W., & Brunetto, G. (2012). Mineralogical changes caused by grape production in a regosol from subtropical Brazilian climate. *Journal of Soils and Sediments*, *12*, 854–862. <https://doi.org/10.1007/s11368-012-0509-x>
- Bortoluzzi, E. C., Pérez, C. A. S., Ardisson, J. D., Tiecher, T., & Caner, L. (2015). Occurrence of iron and aluminum sesquioxides and their implications for the P sorption in subtropical soils. *Applied Clay Science*, *104*, 196–204. <https://doi.org/10.1016/j.clay.2014.11.032>
- Bortoluzzi, E. C., Pernes, M., & Tessier, D. (2008). Mineralogia de partículas envolvidas na formação de gradiente textural em um Argissolo subtropical. *Revista Brasileira de Ciência do Solo*, *32*, 997–1007. <https://doi.org/10.1590/S0100-06832008000300009>
- Bortoluzzi, E. C., & Poletto, C. (2013). Qualidade de sedimentos. In C. Poletto & G. H. Merten (Eds.), *Metodologias para estudo de sedimentos: Ênfase na proporção e na natureza mineralógica das partículas* (2nd ed., pp. 35–90). ABRH.
- Bortoluzzi, E. C., Velde, B., Pernes, M., Dur, J. C., & Tessier, D. (2008). Vermiculite with hydroxy-aluminium interlayer and kaolinite formation in a subtropical sandy soil from south Brazil. *Clay Minerals*, *43*(2), 155–163. <https://doi.org/10.1180/claymin.2008.043.2.03>
- Brown, G., & Brindley, G. W. (1980). X-ray diffraction procedures for clay mineral identification. In G. W. Brindley & G. Brown (Eds.), *Crystal structures of clay minerals and their X-ray identification* (pp. 305–361). Mineralogical Society. <https://doi.org/10.1180/mono-5>
- Caner, L., Radtke, L. M., Vignol-Lelarge, M. L., Inda, A. V., Bortoluzzi, E. C., & Mexias, A. S. (2014). Basalt and rhyo-dacite weathering and soil clay formation under subtropical climate in southern Brazil. *Geoderma*, *235–236*, 100–112. <https://doi.org/10.1016/j.geoderma.2014.06.024>
- Cermeño, P., Falkowski, P. G., Romero, O. E., Schaller, M. F., & Vallina, S. M. (2015). Continental erosion and the Cenozoic rise of marine diatoms. *Proceedings of the National Academy of Sciences*, *112*(14), 4239–4244. <https://doi.org/10.1073/pnas.1412883112>
- Churchman, G. J., & Lowe, D. J. (2012). Alteration, formation, and occurrence of minerals in soils. In P. M. Huang, Y. Li, & M. E. Sumner (Eds.), *Handbook of soil sciences: Properties and processes* (2nd ed., pp. 20.1–20.72). CRC Press.
- Curi, N., & Kämpf, N. (2012). Caracterização do Solo. In J. C. Ker, N. Curi, C. E. G. R. Schaefer, & P. Vidal-Torrado (Eds.), *Pedologia—Fundamentos* (1st ed., pp. 147–169). Sociedade Brasileira de Ciência do Solo.
- da Silva, A. P. R., da Silva, L. J. R., Deus, A. C. F., Fernandes, D. M., & Büll, L. T. (2023). Silicon application methods influence the nutrient uptake of maize plants in tropical soil. *Silicon*, *15*(17), 7327–7334. <https://doi.org/10.1007/s12633-023-02592-3>
- Demattê, J. L. I., Beltrame, J. A., Paggiaro, C. M., & Ribeiro, S. S. (2011). Uso de silicatos em cana-de-açúcar. *Informações Agrônomicas*, *133*, 7–12.
- Demir, S., Alaboz, P., Dengiz, O., Şenol, H., Yilmaz, K., & Başkan, O. (2022). Physico-chemical and mineralogical changes of lithic xerorthent soils on volcanic rocks under semi-arid ecological conditions. *Earth Sciences Research Journal*, *26*(4), 291–301. <https://doi.org/10.15446/esrj.v26n4.96571>
- De Oliveira, J. S., Inda, A. V., Barrón, V., Torrent, J., Tiecher, T., & De Oliveira Camargo, F. A. (2020). Soil properties governing phosphorus adsorption in soils of Southern Brazil. *Geoderma Regional*, *22*, Article e00318. <https://doi.org/10.1016/j.geodrs.2020.e00318>
- De Tombeur, F., Cornelis, J.-T., & Lambers, H. (2021). Silicon mobilization by root-released carboxylates. *Trends in Plant Science*, *26*(11), 1116–1125. <https://doi.org/10.1016/j.tplants.2021.07.003>
- Deus, A. C. F., da Silva, A. P. R., da Silva, L. J. R., de Almeida Bertani, R. M., de Aquino Vidal Lacerda Soares, A., Kano, C., Fernandes, D. M., & Büll, L. T. (2024). Innovations in studies on the quantification of the bioavailability of silicon in the soil. In R. D. M. Prado, H. Etesami, & A. K. Srivastava (Eds.), *Silicon advances for sustainable agriculture and human health: Increased nutrition and disease prevention* (pp. 81–100). Springer.
- Dos Passos, M. G., Do Prado, G. P., Fontana, C., Zonta, E. I., & Bianchini, E. (2021). Natural regeneration in a mixed ombrophilous forest remnant in southern Brazil. *Neotropical Biology and Conservation*, *16*(1), 167–183. <https://doi.org/10.3897/neotropical.16.e58188>
- Ehrenfeld, J. G., Ravit, B., & Elgersma, K. (2005). Feedback in the plant-soil system. *Annual Review of Environment and Resources*, *30*, 75–115. <https://doi.org/10.1146/annurev.energy.30.050504.144212>
- FAO. (2006). *Guidelines for soil description* (4th ed.). FAO.
- Gee, G. W., & Bauder, J. W. (1986). Particle-size analysis. In A. Klute (Ed.), *Methods of soil analysis: Part 1 Physical and mineralogical methods* (2nd ed., pp. 383–411). American Society of Agronomy, Soil Science Society of America. <https://doi.org/10.2136/sssabookser5.1.2ed.c15>
- Gómez, A. R., Riccomini, C., & Fúlfaro, V. J. (2010). Petrography and geochemistry of silicic volcanic rocks of the Paraná volcanic province

- in southern Brazil. *Journal of South American Earth Sciences*, 30(3–4), 168–179.
- Guimarães, C. C. B., Demattê, J. A. M., Azevedo, A. C. D., Silva, R. C. D., & Salazar, D. F. U. (2021). Intemperismo de solos originários de basalto na Bacia do Paraná, São Paulo, Brasil. *Revista Ciência Agrônômica*, 52, Article e20196677. <https://doi.org/10.5935/1806-6690.20210063>
- Henriet, C., De Jaeger, N., Dorel, M., Opfergelt, S., & Delvaux, B. (2008). The reserve of weatherable primary silicates impacts the accumulation of biogenic silicon in volcanic ash soils. *Biogeochemistry*, 90, 209–223. <https://doi.org/10.1007/s10533-008-9245-0>
- Hinsinger, P., Barros, O. N. R., Benedetti, M. F., Noack, Y., & Callot, G. (2001). Plant-induced weathering of a Basaltic Rock: Experimental evidence. *Geochimica et Cosmochimica Acta*, 65(1), 137–152. [https://doi.org/10.1016/S0016-7037\(00\)00524-X](https://doi.org/10.1016/S0016-7037(00)00524-X)
- Hummes, A. P., Inda, A. V., Olk, D. C., & Bortoluzzi, E. C. (2024). Mineral changes in the rhizospheres of conifer plantations for a weathered subtropical soil. *Soil Science Society of America Journal*, 88, 1463–1478. <https://doi.org/10.1002/saj2.20682>
- IBGE. (2015). *Manual técnico de pedologia: Guia prático de campo*. Instituto Brasileiro de Geografia e Estatística.
- IBGE. (2019). *Mapa de biomas e sistema costeiro-marinho do Brasil—1:250 000*. <https://www.ibge.gov.br>
- IUSS Working Group WRB. (2022). *World reference base for soil resources* (4th ed.). International Union of Soil Sciences.
- Korchagin, J., Bortoluzzi, E. C., Moterle, D. F., Petry, C., & Caner, L. (2019). Evidences of soil geochemistry and mineralogy changes caused by eucalyptus rhizosphere. *Catena*, 175, 132–143. <https://doi.org/10.1016/j.catena.2018.12.001>
- Korndörfer, G. H., Pereira, H. S., & Nolla, A. (2004). *Análise de silício: Solo, planta e fertilizante* (Boletim Técnico 2). GPSi/ICIAG/UFU.
- Mamasolieva, M., Gafurova, L., Hudoyazarov, I., & Juliev, M. (2024). Role of silicon and silicon fertilizers in the world: A review of papers from the Scopus database published in English for the period of 2012–2022. *Soil Science Annual*, 75(1), Article 186456. <https://doi.org/10.37501/soilsa/186456>
- Melo, V. F., Corrêa, G. F., Maschio, P. A., Ribeiro, A. N., & Lima, V. C. (2003). Importância das espécies minerais no potássio total da fração argila de solos do Triângulo Mineiro. *Revista Brasileira de Ciência do Solo*, 27, 807–819. <https://doi.org/10.1590/S0100-06832003000500005>
- Melo, V. F., Schaefer, C. E. G. R., Novais, R. F., Singh, B., & Fontes, M. P. F. (2002). Potassium and magnesium in clay minerals of some Brazilian soil as indicated by a sequential extraction procedure. *Communications in Soil Science and Plant Analysis*, 33(13–14), 2203–2225. <https://doi.org/10.1081/CSS-120005757>
- Meunier, A., Caner, L., Hubert, F., El Albani, A., & Pret, D. (2013). The weathering intensity scale (WIS): An alternative approach of the chemical index of alteration (CIA). *American Journal of Science*, 313, 113–143. <https://doi.org/10.2475/02.2013.03>
- Meunier, A., Sardini, P., Robinet, J. C., & Prêt, D. (2007). The petrography of weathering processes: Facts and outlooks. *Clay Minerals*, 42, 415–435. <https://doi.org/10.1180/claymin.2007.042.4.01>
- Nardy, A. J. R., Macedo, M. H. F., Wildner, W., & Fonseca, M. A. (2002). Depósitos Vulcânicos Ácidos da Bacia do Paraná: Caracterização e evolução. *Geologia USP. Série Científica*, 2(1), 29–42.
- Oliveira, T. E. D., Freitas, D. S. D., Gianezini, M., Ruviaro, C. F., Zago, D., Mércio, T. Z., Dias, E. A., Lampert, V. D. N., & Barcellos, J. O. J. (2017). Agricultural land use change in the Brazilian Pampa Biome: The reduction of natural grasslands. *Land Use Policy*, 63, 394–400. <https://doi.org/10.1016/j.landusepol.2017.02.010>
- Pujar, K. G., Hiremath, S. C., Pujar, A. S., Pujeri, U. S., & Yadawe, M. S. (2012). Analysis of physico-chemical and heavy metal concentration in soil of Bijapur Taluka, Karnataka. *Scientific Reviews and Chemical Communications*, 2(1), 76–79.
- Puppe, D., Kaczorek, D., Stein, M., & Schaller, J. (2023). Silicon in plants: Alleviation of Metal(loid) toxicity and consequential perspectives for phytoremediation. *Plants*, 12, Article 2407. <https://doi.org/10.3390/plants12132407>
- Schaetzl, R. J., & Anderson, S. (2005). *Soils: Genesis and geomorphology*. Cambridge University Press. <https://doi.org/10.1017/CBO9780511815560>
- Soil Survey Staff. (2022). *Keys to soil taxonomy* (13th ed.). USDA-NRCS.
- Stockmann, U., Minasny, B., & McBratney, A. B. (2014). How fast does soil grow? *Geoderma*, 216, 48–61. <https://doi.org/10.1016/j.geoderma.2013.10.007>
- Strömberg, C. A. E., Di Stilio, V. S., & Song, Z. (2016). Functions of phytoliths in vascular plants: An evolutionary perspective. *Functional Ecology*, 30, 1286–1297. <https://doi.org/10.1111/1365-2435.12692>
- Tale, K. S., & Ingole, S. (2015). A review on role of physico-chemical properties in soil quality. *Chemical Science Review and Letters*, 4(13), 57–66.
- Teixeira, P. C., & Campos, D. V. B. (2017). Relações moleculares Ki e Kr. In P. C. Teixeira, G. K. Donagemma, A. T. Fontana, & W. G. Teixeira (Eds.), *Manual de métodos de análise de solo* (3rd ed., pp. 286–287). Embrapa Solos.
- Teixeira, P. C., Donagemma, G. K., Fontana, A., & Teixeira, W. G. (Eds.). (2017). *Manual de métodos de análises de solo* (3rd ed.). EMBRAPA.
- Tubana, B. S., Babu, T., & Datnoff, L. E. (2016). A review of silicon in soils and plants and its role in US agriculture: History and future perspectives. *Soil Science*, 181(9–10), 393–411. <https://doi.org/10.1097/SS.0000000000000179>
- White, A. F., Vivit, D. V., Schulz, M. S., Bullen, T. D., Evett, R. R., & Agarwal, J. (2012). Biogenic and pedogenic controls on Si distributions and cycling in grasslands of the Santa Cruz soil chronosequence, California. *Geochimica et Cosmochimica Acta*, 94, 72–94. <https://doi.org/10.1016/j.gca.2012.06.009>
- Zabowski, D., & Ugolini, F. C. (1992). Seasonality in the mineral stability of a subalpine Spodosol. *Soil Science*, 154, 497–504. <https://doi.org/10.1097/00010694-199212000-00009>
- Zaman, W., Ayaz, A., & Puppe, D. (2025). Biogeochemical cycles in plant–soil systems: Significance for agriculture, interconnections, and anthropogenic disruptions. *Biology*, 14(4), Article 433. <https://doi.org/10.3390/biology14040433>

**How to cite this article:** Dalacorte, L., da Silva, A. P. R., Fernandes, D. M., & Bortoluzzi, E. C. (2025). Influence of vegetation type on silicon content in different subtropical soils. *Soil Science Society of America Journal*, 89, e70107. <https://doi.org/10.1002/saj2.70107>